Stability and Migration of Metal Ions in G4-Wires by Molecular Dynamics Simulations

Manuela Cavallari,*,† Arrigo Calzolari,† Anna Garbesi,†,‡ and Rosa Di Felice*,†

National Center on nanoStructures and bioSystems at Surfaces (S3) of INFM-CNR, Dipartimento di Fisica, Università di Modena e Reggio Emilia, Via Campi 213/A, 41100 Modena, Italy and CNR-ISOF, Area della Ricerca, Via P. Gobetti 101, 40129 Bologna, Italy

Received: July 17, 2006; In Final Form: October 6, 2006

We present a molecular dynamics investigation of guanine quadruple helices based on classical force fields. We analyze the dependence of the helical conformation on various compositional factors, such as the length of the G4-wire, as well as the incorporation into the helix channel of alkali ions of different species and in different amounts. In compliance with previous indications, our results suggest that monovalent alkali cations assist the stability of the quadruplex arrangement against disruption on the few nanoseconds time scale in the order of increasing van der Waals radius. Whereas very short G4-wire fragments immediately unfold in the absence of coordinating metal ions or in the presence of tiny ions (e.g., Li^+) in agreement with the experimental evidence that empty short guanine quadruplexes are not formed in any synthetic conditions, our simulations show that longer empty helices do not discompose. This finding supports the possibility of producing long G4-wires with different guanine-cation stoichiometries than those routinely known. The classical trajectories allow us to identify different stationary axial sites for the different metal species, which are confirmed by complementary quantum calculations.

1. Introduction

The G-quartet is a planar macrocycle formed by the assembly of four guanines held together by eight hydrogen bonds, four internal and four external (Figure 1b). It is the fundamental building block of the supramolecular structures formed: (i) by oligoguanylates and G-rich oligonucleotides in water[1] and (ii) by lipophilic derivatives of guanosine in organic solvents.[2] All such supramolecular objects are characterized by the presence of a helical stack of the basic tetrameric unit and of a row of cations filling the central cavity.[1−5] Depending on their size, the cations are coplanar with G-quartets or sandwiched between them. In fact, with one notable exception,[6] all the self-assembly processes leading to the G-quartets and G-quadruplexes described thus far occur only in the presence of suitable cations, which are deemed essential for both templation and stabilization of this type of ordered supramolecular aggregates.

The ability of guanosine derivatives to self-associate was first reported in 1910,[7] and the G-quartet structure was identified in 1962.[8] In 1988, it was found that synthetic oligonucleotides, containing short G-rich sequences present in the immunoglobulin switch regions, self-associate at physiological salt concentration to give four stranded structures.[9] Because stretches of adjacent guanosines are present in several chromosomal locations, G-quadruplexes were proposed to play a role in several biological processes, in particular those governing telomere function. By now, the interest for the structures formed by the self-assembly of a variety of guanosine derivatives has become very wide, going from molecular biology to nanotechnology, as described in the excellent review by Davis.[3] The very structure of the G-quadruplex suggests that it may sustain the motion of ions in the inner channel.[4] Indeed, it was estimated, by an indirect method, that at 283 K the lifetime of sodium cations bound within the central cavity of a four G-quartet stack is 250 μs.[10] With the same quadruplex, it was found that ammonium cations move instead between the channel and the solution with a much longer residence time of 250 ms in the most inner coordination site.[11] It was suggested that the much larger mobility of sodium is due to its small ionic radius (0.97 Å), which allows it to move "freely'' along the central cavity, while the larger ionic radius of ammonium (1.43 Å) requires that the G-quartet partially opens or assumes altered conformations to permit its movement between the coordination sites.[12] Inspired by these findings, we decided to undertake molecular dynamics (MD) simulations of G-quadruplexes. Notwithstanding the limited time scales accessible with such a theoretical tool that inhibit a direct probing of ion transit times, we wanted to understand if and to which extent MD trajectories are still able to capture differences both in the mobility of cations with different ionic radius within the channel of G-quadruplexes and in their influence on the structural rigidity/flexibility of the G-quartet planes and of the overall helix.[13] To this purpose, we simulated the behavior of G-quadruplexes containing 9 G-quartets and various species and amounts of alkali cations for 5 ns.

The second aim of our work was to study with the same tool the dynamics of G-quadruplexes without coordinated cations in the inner cavity. MD simulations by different authors demonstrated deformation of the quadruple helical conformation in the absence of internal cations or for partially coordinated G-quadruplexes containing from 4 to 7 G-quartet planes.[13−18] Our interest for "empty'' G-quadruplexes was motivated by a preliminary observation[19,20] that long homodeoxyguanylates self-assemble to give stable, monomolecular G-quadruplexes in solutions containing only the Tris(hydroxymethyl)aminomethane cation, whose size does not allow it to fit within the channel.

* Corresponding Authors. (R.D.F.) Phone: +39-059-2055320. Fax: +39-059-2055651. E-mail: rosa@unimore.it. (M.C.) E-mail: cavallari.manuela@unimore.it.

† National Center S3 INFM-CNR.

‡ CNR-ISOF.

10.1021/jp064522y CCC: $33.50
Published on Web 11/24/2006

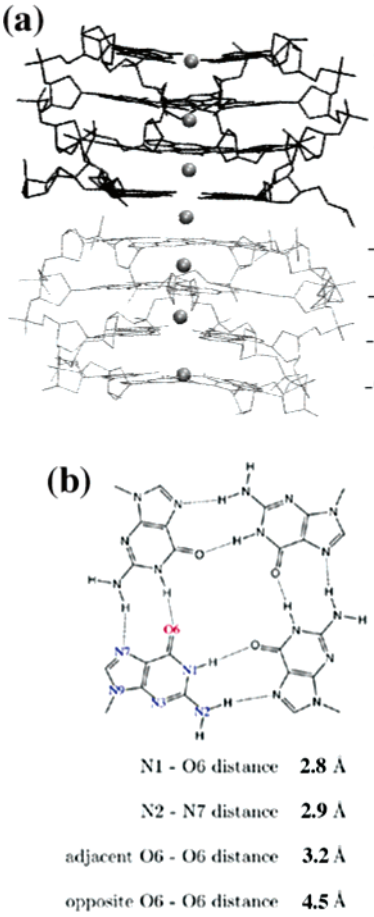

Figure 1. (a) The X-ray resolved crystal structure of parallel-stranded guanine-quadruplex $d(TG_4T)_2$ molecules at 0.95 Å resolution.[5] The unit cell consists of four 4-plane G4-wires. Any two G4w's stack on top of each other with opposite polarity with the interface formed by their 5′ ends. Sodium ions inside the G-channel are indicated by spheres. For clarity, water molecules and thymine bases are not shown. The four uppermost guanine tetramers (dark) and ions constitute the reference structure for this work. (b) The building-block planar guanine tetramer, G4t; the "double ring" of H-bonds is clearly shown.

Hence, we carried out 5 and 20 ns MD simulations on G-quadruplexes containing 9 and 24 G-quartets, respectively, in the absence of coordinated cations in the initial structure; these choices tackle longer polymers than what was done in the past.[13−18]

The paper is organized as follows. First we present and discuss the results of the classical MD simulations in section 2: the method and computational setup are described in sections 2.1 and 2.2; then, the results are presented in sections 2.3 to 2.5 and discussed in section 2.6. To investigate more thoroughly the cation stability sites identified by the classical trajectories and to attain a rough estimation of the relative energy barriers between metastable ionic sites along the helix, we also performed quantum calculations based on density functional theory (DFT), whose results are presented in section 3. Finally, we summarize our work in section 4.

2. Molecular Dynamics Simulations

2.1. Method. All the MD simulations discussed in this work were carried out using the NAMD[21] program with the AMBER force field as parametrized by Cornell et al.[22] The main motivation for our choice of NAMD was the better scalability on parallel supercomputers that are needed to simulate the large structures that we present. The nucleic acid molecules were explicitly solvated with a buffer of 10 Å of water molecules using the TIP3P model.[23] The number of water molecules included in the simulations varied approximately between 4000 and 7000, depending on the size of the solute molecule. Periodic boundary conditions (PBC) were applied. The translational motion of the center of mass was periodically removed. The shape of the unit cell was orthorhombic with sizes dependent on the simulated system. We verified that the chosen sizes are such that neighboring replicas did not interact (more details in section 2.2). The total charge of the system was neutralized by an appropriate number of Li^+, Na^+, or K^+ cations (see later), using standard parameters of the force field: the van der Waals radius in Å was 1.137, 1.868, and 2.658, and the well depth in kcal/mol was 0.0183, 0.00277, and 0.000328, for Li^+, Na^+, and K^+, respectively.[22]

We used the following standard protocols for both the equilibration and production molecular dynamics. The bond between each hydrogen and its mother atom was fixed to the nominal bond length by means of the SHAKE[24] procedure. A 9.0 Å cutoff was applied to the Lennard-Jones interactions, while the electrostatic interactions were computed using the particle mesh Ewald method[25] (PME) to avoid their truncation in the calculations. The PME charge grid spacing was less than 1 Å. The charge grid was interpolated using a cubic B-spline with a direct sum tolerance of 10^{-6} at the 9 Å direct space cutoff. A time step of 2 fs was used.

The simulation of each system was characterized by a minimization-equilibration phase followed by production molecular dynamics in which the system coordinates were collected every 1 ps. The conjugate gradient[26] method was used for the system minimization. Because the positions of solvent atoms were initially assigned according to standard rules[27] around the quadruple helices (which instead were constructed from the PDB file[5]), we initially performed solvent equilibration only. In this MD stage, all the water molecules and cations were subjected to 20 ps dynamics, keeping the nucleic acid molecules fixed with a SHAKE[24] tolerance of 10^{-8}. The temperature of the solvent molecules was slowly raised to 100 K by coupling them to a heat bath, and the pressure was kept at 1.01325 bar (atmospheric pressure at sea level) using the Berendsen method.[28] Second, after a further all-system minimization, the quenched system was heated slowly from 0 to 300 K, by coupling it to a heat bath whose temperature was raised at the rate of 50 K every 10 ps. Finally, the system was equilibrated 100 ps longer, before starting the production MD during which the system temperature and pressure were kept constant at 300 K and 1.01325 bar, respectively. The temperature was maintained through the addition of friction and random forces in a Langevin dynamics[29] scheme. A modified Nosé−Hoover[30] method in the context of Langevin dynamics controlled the fluctuations in the barostat. Thus, the multi ns MD simulations were performed in the NPT ensemble (constant number of particles, pressure, and temperature). We assigned a damping coefficient of 1 ps^{-1} for the Langevin dynamics of each atom, while the barostat was characterized by an oscillation time period of 200 fs, by a decay time of 100 fs and by a noise temperature of 300 K for the Langevin piston method.

Overall rotations and translations were removed from the trajectories with the method introduced by Kneller[31] within the formalism of quaternion algebra to enable the direct comparison of different systems. The analysis of the trajectories is focused on the two following properties.

2.1.1. Mean Square Displacements. The relative motion of the G4-wires (G4w's) during the simulation was described by

TABLE 1: Summary of Simulations Carried out in This Work

starting structure	cations[a]	main purpose of the simulation	length[b] (ns)	label
X-ray, 4 planes	3 Na^+ (Na^+)	method validation	3.0	
X-ray, 4 planes	2 Na^+ (Na^+)	method validation	3.0	
X-ray, 4 planes	(Na^+)	method validation	3.0	
model, 9 planes	9 Li^+ (Li^+)	cation role in structure and stability, hydration	5.0	9Li9P
model, 9 planes	8 Na^+ (Na^+)	cation role in structure and stability, hydration	5.0	8Na9P
model, 9 planes	8 K^+ (K^+)	cation role in structure and stability, hydration	5.0	8K9P
model, 9 planes	1 Li^+ (Li^+)	water role in structure and stability	5.0	1Li9P
model, 9 planes	(Na^+)	water role in structure and stability	5.0	9P
model, 24 planes	(Li^+)	structure and stability of long G4w's	20.0	24P

[a] Number and species of internal cations (species of external counterions). [b] Duration of the production MD runs.

the root-mean-square displacements (RMSDs) from chosen reference structures. A linear measure is the time-dependent RMSD value that gives the deviation of the molecular coordinates at time t from the average structure taken over an interval T, that is

$$\mathrm{RMSD}(t) = \left[\frac{1}{N}\sum_{i=1}^{N}[\mathbf{r}_i(t) - \langle \mathbf{r}_i\rangle_T]^2\right]^{1/2} \quad (1)$$

where $\mathbf{r}_i(t)$ are the coordinates of the i-th atom at time t, $\langle \mathbf{r}_i\rangle_T$ are the average coordinates of the i-th atom evaluated over the time span T, and N is the number of atoms in the domain of interest. The averaging interval T for each structure is specified later along with the presentation of the results. The results are analyzed both as a function of time (Supporting Information) and in terms of occurrence probability. In addition, to bypass the general ill-definition of the mean-square displacements in some circumstances (e.g., bimodal distributions), we compute unbiased mean-square displacements of the atoms using a technique[32] inspired by the analysis of the variance. In brief, this method consists of the following steps: (i) dividing the whole simulation time in n "blocks" and performing "within-blocks" averages of the linear and squared atomic positions, $\langle x_i\rangle^j$ and $\langle x_i^2\rangle^j$, over such finite time intervals rather than over the whole trajectory; (ii) defining the within-blocks atomic mean square displacement (MSD) for atom i as

$$\langle u_i^2\rangle_{\mathrm{wb}} = \frac{1}{3n}\sum_{j=1}^{n}[\langle x_i^2\rangle_j - \langle x_i\rangle_j^2 + \langle y_i^2\rangle_j - \langle y_i\rangle_j^2 + \langle z_i^2\rangle_j - \langle z_i\rangle_j^2] \quad (2)$$

where the subscript wb stands for within-blocks; (iii) analyzing the variability of the resulting MSD distribution of all the base atoms to the extent of the blocks on which the averages are computed; (iv) selecting from the test (iii) the block extent for which there is a sort of plateau of the relevant index; and (v) performing the distribution analysis for the selected block width. The reader is referred to the original work for more details.[32] After Maragliano and co-workers,[32] we performed the χ^2 test on the structure 8K9P (Supporting Information, label defined in Table 1) and determined the optimal block width of 100 ps. We used this same block width for all the structures.

2.1.2. Hydrogen Bonds (HBs). We inspect the distribution (center and spreading) of the standard N1—O6 and N2—N7 bonds (Figure 1b) and compare the average lengths and angles to reference crystal structure data:[2,3,5] d(N1—6) ≃ d(N2—N7) ≃ 2.9 Å, Θ (N1—O6) ≃ 162°, Θ (N2—N7) ≃ 169°. We briefly comment on the occurrence of nonstandard N1—N7 and N2—O6, previously noted by other authors.

2.2. Starting Structures. Starting atomic models are based on the X-ray crystal structure of the $d(TG_4T)_4$ quadruplex at 0.95 Å resolution.[5] Four guanine-quadruplex $d(TG_4T)$ fragments (A, B, C, D) exist in the unit cell of this crystal phase. Tetraplex B, including four sodium cations inside the G-channel, is taken as reference for this study (see test simulation in the Supporting Information). Figure 1a displays half of the crystal unit cell with two $d(TG_4T)$ fragments of opposite polarities, located one on top of the other. Figure 1b shows a top view of a single plane, the G4-tetrad (G4t). From now on, we will name G4w any stack of G4ts characterized by the crystallographic parameters (rise and twist of the helix) as in the $d(TG_4T)_4$ crystal, although in principle the name G4-wire should apply only to long helices.

For the construction of the G4ws with 9 and 24 G4t's, the first tetrad (set at the 5′ end) is taken from the above mentioned X-ray structure, choosing the one with the four G-bases lying as much as possible on the same plane, namely G2 in Figure 1a. The other tetrads are built by subsequent rotations of 30° and translations of 3.37 Å of the G2-plane, according to the crystallographic parameters. In these model structures, the terminal thymines are omitted. After solvation, the edges of the unit cell range around 50 Å in the directions perpendicular to the quadruplex axis and around 50 and 100 Å along the helix axis for the 9- and 24-plane quadruplexes, respectively. For each G4w, the cations are positioned both inside and outside the channel. The external cations, which play the role of counterions, are initially placed in the most negative locations around the G4w backbone. The internal cations are manually added into the G-channel: the K^+ and Na^+ ions are positioned between consecutive G4ts, each coordinated with eight O6 oxygens (interplane position); the Li^+ ions are located in the center of each tetrad, each coordinated with four O6 oxygens (intraplane position). Globally, 32 and 92 monovalent ions neutralize the charge of the 9- and 24-plane quadruplexes, respectively.

The interplane arrangement of the sodium cations was found in the inner G4t's of the X-ray structure.[5,33] Because potassium has a larger ionic radius than sodium, it is unlikely that K^+ ions could adopt intraplane positions. Besides this consideration, an experimental evidence also supports this choice for the location of K^+ ions: X-ray study of a K^+ stabilized G4w[34] (a $d(G_4T_4G_4)$ dimer) detected a single cation located between the central pair of G4ts. On the other hand, the small ionic radius of lithium suggests that Li^+ ions would select intraplane positions, and this is our starting choice. Constraints are not applied; therefore, adjustments of the cation positions during the simulation are allowed, including drifts from an intraplane site to an interplane site, and vice versa.

Let us define a "cation fully coordinated" G4w as a quadruple helical stack of n G4t's that incorporates the maximum number of possible inner cations, namely n-1 interplane ions or n intraplane ions. Similarly, "cation partially coordinated' G4ws are tetrad stacks that coordinate a number of inner cations less than the highest possible number. Besides cation fully coordinated G4w's, we also simulated cation partially coordinated and empty G4ws. Table 1 summarizes all the simulations carried

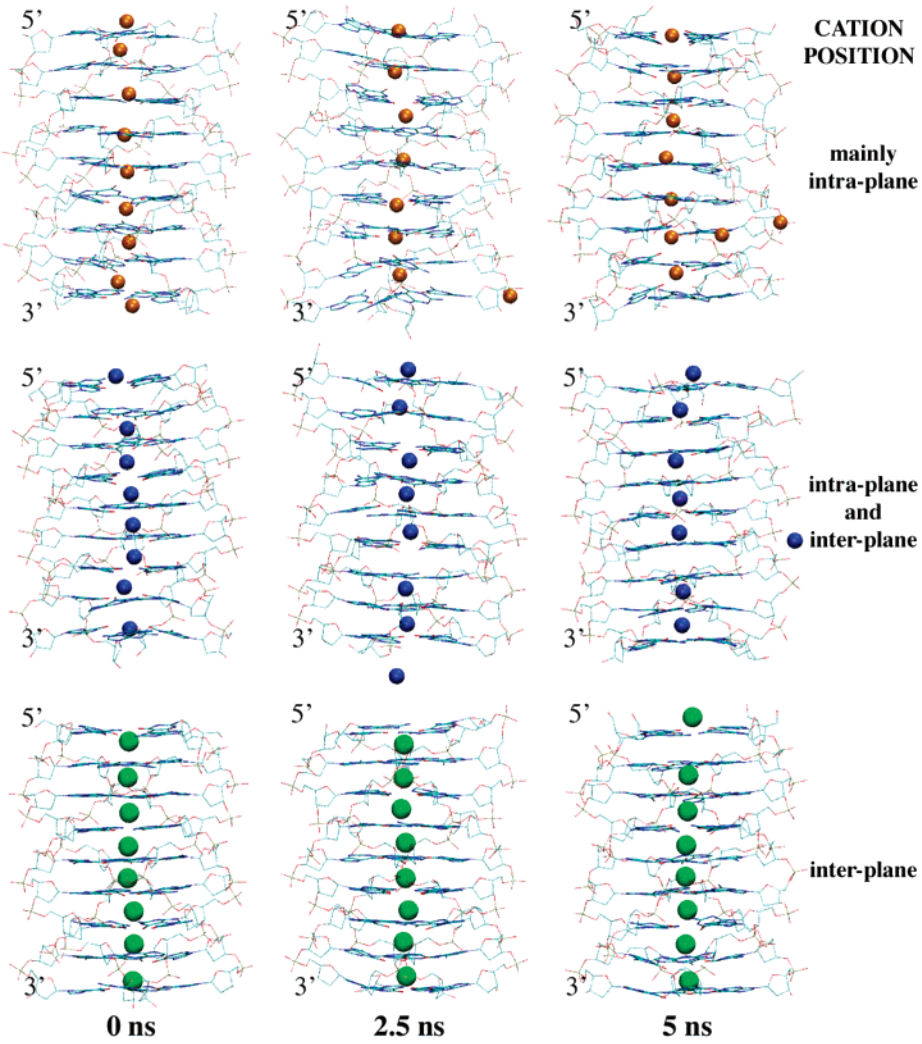

Figure 2. MD snapshots at 0 ns (equilibrated structure), 2.5, and 5 ns of the cation fully coordinated G4w's composed of nine tetrameric planes. Snapshots in the top row correspond to the 9Li9P structure (initial geometry in Supporting Information, Figure S1d), those in the middle row to 8Na9P (initial geometry in Supporting Information, Figure S1e), and those in the bottom row to 8K9P (initial geometry in Supporting Information, Figure S1f). The cations are shown as spheres of different colors: Na^+, K^+ and Li^+ cations are colored in blue, green and orange, respectively. The cations that leave the G-channel and remain in its vicinity within 3.0 Å also are visualized. The structural labels are defined in Table 1.

out in this work (a schematic description of the initial structures is drawn in the Supporting Information, Figure S1).

The force field adopted here[22] was extensively applied in studies of four-stranded nucleic acids[13−17,35−39] within the MD code AMBER.[40] Hence, a preliminary part of our work, reported in the Supporting Information, is devoted to testing the performance and accuracy of the NAMD code to describe the system of interest by a gross comparison to results obtained with other MD codes.[14] For these initial tests, we simulate the key tetramer d(TG_4T) whose X-ray crystal structure was solved.[5] We use the short oligomers only as test cases and then proceed further to longer quadruplexes, which are recently being synthesized and characterized.[20]

2.3. Cation Fully Coordinated 9-Plane G4w's. In Figure 2, we show the structures of the 9Li9P, 8Na9P, and 8K9P G4ws at 0, 2.5, and 5.0 ns, from the 5 ns MD production runs. The MD average structures are shown in Figure 3(a−c). A glance at Figures 2 and 3 reveals that the quadruplex symmetry, namely coplanar and equispaced G4ts, is highly maintained in fully coordinated G4ws. The larger the ion size is (Li^+ < Na^+ < K^+), the more the regular quadruplex conformation is maintained.

In the equilibrated 9Li9P, the Li^+ ions in the inner part of the helix persist at their original in-plane positions, while those near the 3′ and 5′ extremes of the G-channel move outward; they indeed leave the tube before the first ns of the simulation. In the following 4 ns of equilibrated simulation, the Li^+ cations that remain inside the channel preserve almost exactly the intraplane coordination, as can be seen from both the subsequent snapshots of Figure 2 and the average structure of Figure 3a.

In the simulation of the 8Na9P G4w, after nearly 2.5 ns the Na^+ cation in 3′ leaves the G-channel. The three innermost Na^+ cations remain at their original interplane sites, while those at the 3′ and 5′ ends occupy new interplane sites shifted toward the G-channel ends (Figure 2). Figure 3b reveals that on the average, Na cations also explore intraplane sites during the time evolution.

All the K^+ cations in 8K9P persist in their original interplane positions during almost the entire simulation. Only during the last ns, the K^+ in 5′ is shifted beyond the 5′ G4t. By continuing this simulation 2 ns longer, we observe that this ion finally abandons the G-channel, while the others keep their positions unaltered.

In 8Na9P and 8K9P, the cations that exit the G-channel spend some time around the edges before leaving the inner core region. This is possible because some coordinated water molecules are positioned immediately beyond the G-terminals. As expected,

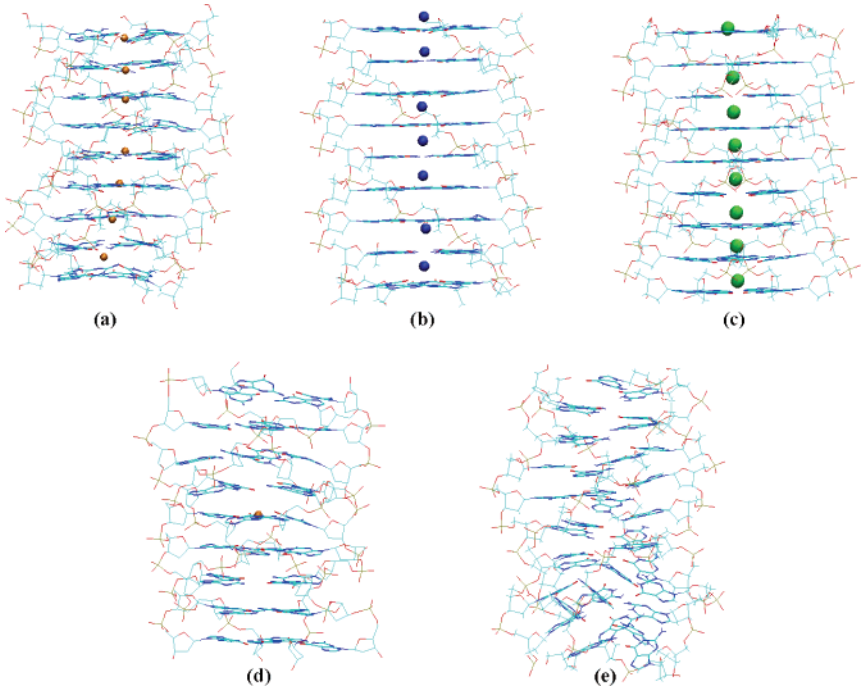

Figure 3. MD average structures of the fully coordinated (a−c) and undercoordinated (d, e) 9-plane G4w's: (a) 9Li9P, (b) 8Na9P, (c) 8K9P, (d) 1Li9P, and (e) 9P. Each average structure is computed over the final 3.5-ns interval of the 5-ns simulation and is taken as reference for the statistical analysis of the RMSDs and of the variances.

the mobility of the cations once they are outside the G-channel is higher than inside. None of the external cations enter the G-channel.

In Figure 4, we show the RMSD (eq 1) and MSD (eq 2) distributions of all the relevant configurations with only the guanine atoms taken into account. The corresponding peak values and standard deviations are given in Table 2. The RMSD signal is computed through eq 1 for each structure relative to the average structure evaluated over the final 3.5 ns span of the 5 ns simulation in which the time dependence of the RMSD relative to the equilibrated structure shows a somehow flat profile (Supporting Information, Figure S3). In this kind of analysis, the peak position and its width for each structure are significant. The RMSD distributions for all the fully coordinated 9-plane G4w's that we simulated are peaked around similar values and have roughly the same spread. The mean RMSD is slightly smaller for the 8K9P structure, indicating an overall major regularity, but there is no strong difference among these structures. The statistical analysis of the MSD distribution, in which the statistics are not taken over the occurrence in time but over the occurrence among all the atoms, confirms these observations.

In Figure 5, we plot the distributions of the HB lengths and angles (N1—O6 and N2—N7) in the various simulated G4-wires. The corresponding average values and standard deviations are reported in Table 3. The N1—O6 and N2—N7 HBs are the standard Hoogsteen HBs found in the X-ray resolved structures in the presence of sodium cations inside the G-channel.[5,33] We note that all the HB lengths experience during the equilibration time a general increase with respect to the crystal structure averages; the different solvation environments in solution and in the crystal phase may be partly responsible for this evidence, although numerical details may also contribute. As a consequence of the HB length variation, the obtained mean values during the dynamical evolution are systematically larger than those in the crystal phase.[2,5] Looking only at the fully coordinated structures (first 3 rows in Table 3), one notes that the bond length increase, and the deviation from the flat angle

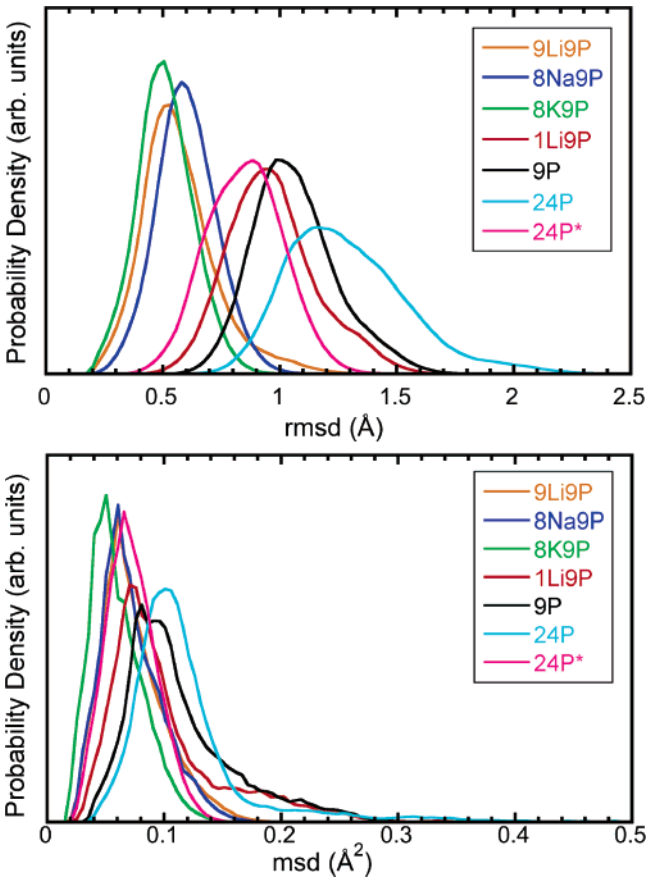

Figure 4. Top: distribution of the RMSD computed from the average structure for various analyzed G4-wires. Bottom: distribution of the variance computed according to Maragliano et al.[32] The legends identify the G4-wires, according to the nomenclature in Table 1. The curves represent convolutions of the histograms. The histograms are reported for preciseness in the Supporting Information.

are remarkable for the "internal'' N1—O6 bonds and less pronounced for the "external'' N2—N7 bonds; we interpret this

TABLE 2: Summary[a] of the Statistical Analysis Performed on the Root and Atomic Mean Square Displacements for All the Simulated G4-Wires

structure	RMSD[b]-eq[c] (Å)	RMSD[b]-av[d] (Å)	MSD[e] (10^{-2} Å^2)
8K9P	0.6 ± 0.1	0.5 ± 0.1	5.4 ± 1.6
8Na9P	0.9 ± 0.1	0.6 ± 0.1	6.7 ± 2.0
9Li9P	1.1 ± 0.1	0.6 ± 0.1	6.9 ± 2.2
1Li9P	1.4 ± 0.5	1.0 ± 0.2	9.7 ± 4.8
9P	2.2 ± 0.5	1.0 ± 0.2	11.0 ± 4.3
24P	2.8 ± 0.5	1.3 ± 0.2	11.6 ± 5.2
24P*	1.3 ± 0.2	0.8 ± 0.1	6.8 ± 1.4

[a] (Peak value) ± (standard deviation). [b] RMSDs computed by summing over the heavy atoms (C, N, O) of guanines. [c] RMSD with respect to the equilibrated structure. [d] RMSD with respect to the average structure. The average structure of 9-plane G4-wires is computed over the final 3.5-ns time interval of the whole 5-ns simulation. The average structure of 20-plane G4-wires is computed over the final 12-ns time interval of the whole 20-ns simulation. [e] As defined in eq 2 according to Maragliano et al.[32]

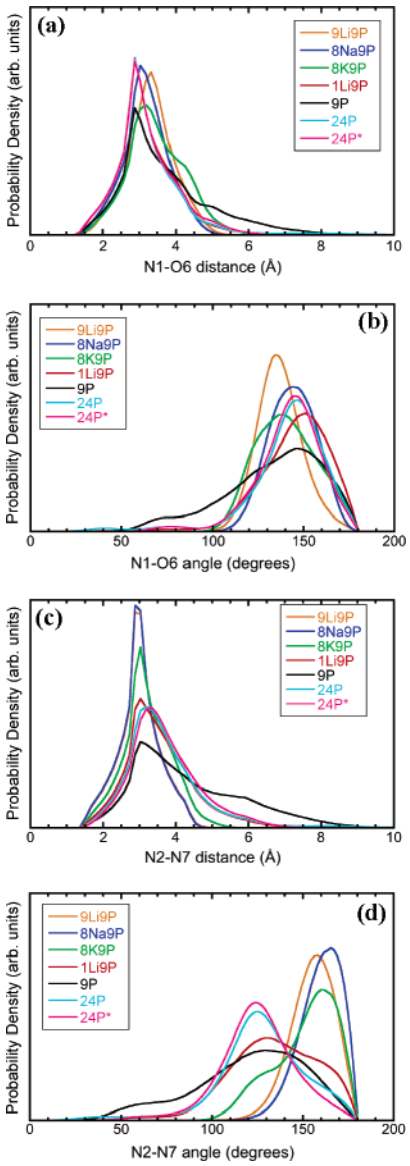

Figure 5. Distribution of H-bond lengths and angles, as identified in the legends and the axis labels. The curves represent convolutions of the histograms. The histograms are reported for preciseness in the Supporting Information.

evidence as the fact that the inner HBs are particularly sensitive to the presence and relaxation of several internal cations. The N1—O6 bond length increases with the cation size (compare 8K9P, 8Na9P, and 9Li9P in Table 3); the slight discrepancy to this rule for 9Li9P and 8Na9P is due to the different coordination sites of the sodium and lithium cations (Na ions are interplanar, and Li ions are intraplanar).

The formation of unusual N1—N7 and N2—O6 bonds was observed and discussed in previous theoretical works.[14,16,41] Nonstandard N2—O6 HBs are not detected by us in the cation fully coordinated G4ws. Nonstandard N1—N7 HBs are formed instead with an abundance that is dependent on the cation species. The weakening of the standard N2—N7 Hoogsteen HBs and the formation of nonstandard N1—N7 HBs is a consequence of an in-plane rotation of the G4t's with respect to the crystal structure. The rotation is shown in Figure 6 in which the central tetrad of the 9Li/8Na/8K9P average structures is superimposed to the central tetrad of the starting configuration.

Two other important indexes of the well-characterized quadruplex structural motif[5,33] are the G-channel size and the stacking distance between consecutive G4t's. The G-channel size may be defined in terms of the distances between adjacent oxygens and between opposite oxygens in each layer (Figure 1b). For this calculation, we consider only the five G4t's in the inner part of the G4w's to neglect border effects. The distance between adjacent O6 atoms has an average value of 3.0 Å and a standard deviation of 0.3 Å, irrespectively of the cation type (compare to the value in Figure 1b). Also, the average distance between opposite O6 atoms does not change significantly when changing the cation species (4.1 ± 0.5 Å for 9Li9P, 4.2 ± 0.4 Å for 8Na9P, 4.2 ± 0.2 Å for 8K9P). Overall, the size of the channel in fully coordinated 9-plane G4w's is practically insensitive to the cation species. The stacking distance is computed as the distance between the centers of mass of two consecutive tetrads. In the 8K9P, 8Na9P, and 9Li9P quadruplexes the stacking distance between any two planes is systematically smaller than the crystallographic value of 3.4 Å. The average stacking distance over all of the nine planes is 3.23 ± 0.02 Å, 3.15 ± 0.02 Å, and 3.20 ± 0.02 Å for 9Li9P, 8Na9P, and 8K9P, respectively.

2.4. Cation Partially Coordinated and Empty 9-Plane G4w's. The MD snapshots of the G4w's with one central (1Li9P) and without (9P) monovalent Li cations are illustrated in Figure 7 at 0, 2.5, and 5 ns of the production MD runs, along with the average structures in Figure 3d, e. Also for these undercoordinated quadruplexes, as for the fully coordinated ones, none of the initial external cations reaches the G-channel. Instead, several water molecules progressively fill the G-channel during the dynamics, entering from both the 3′ and 5′ openings. The internal Li^+ ion in 1Li9P remains at its initial intraplane location. The low cation concentration in the 1Li9P G-channel makes the structure extremely flexible, as shown in the snapshots of Figure 7, especially in the 3′ border, but the symmetry of the G4w is on average conserved and no permanent deviation from the quadruplex arrangement is found (see Figure 3d). On the contrary, the absence of any coordinated cations not only

TABLE 3: Summary[a] of the Statistical Analysis Performed on the H-bond Lengths and Angles for All the Simulated G4-wires

structure	N1−O6 (Å)	N1−H1−O6 (deg)	N2−N7 (Å)	N2−H21−N7 (deg)
8K9P	3.5 ± 0.5	140.4 ± 15.5	3.2 ± 0.4	151.7 ± 16.7
8Na9P	3.2 ± 0.3	144.1 ± 11.7	3.0 ± 0.1	160.4 ± 10.4
9Li9P	3.3 ± 0.3	136.8 ± 10.9	3.0 ± 0.2	155.8 ± 10.9
1Li9P	3.2 ± 0.7	145.0 ± 19.1	3.5 ± 0.9	133.6 ± 24.3
9P	3.7 ± 1.1	133.2 ± 26.4	4.3 ± 1.4	120.5 ± 30.1
24P	3.3 ± 0.9	141.1 ± 22.4	3.7 ± 1.1	126.4 ± 24.7
24P*	3.2 ± 0.6	141.5 ± 18.0	3.7 ± 0.8	124.7 ± 20.2
1Li9P (central tetrad)	3.0 ± 0.1	150.8 ± 9.1	2.9 ± 0.1	164.1 ± 8.5
1Li9P (terminal tetrads)	3.6 ± 1.2	135.4 ± 27.1	4.0 ± 1.3	123.6 ± 31.7
crystal data[b]	∼2.9	∼162	∼2.9	∼169

[a] (Peak value) ± (standard deviation). [b] These values are averaged among the various tetrads composing lipophilic guanine quadruplexes.[2]

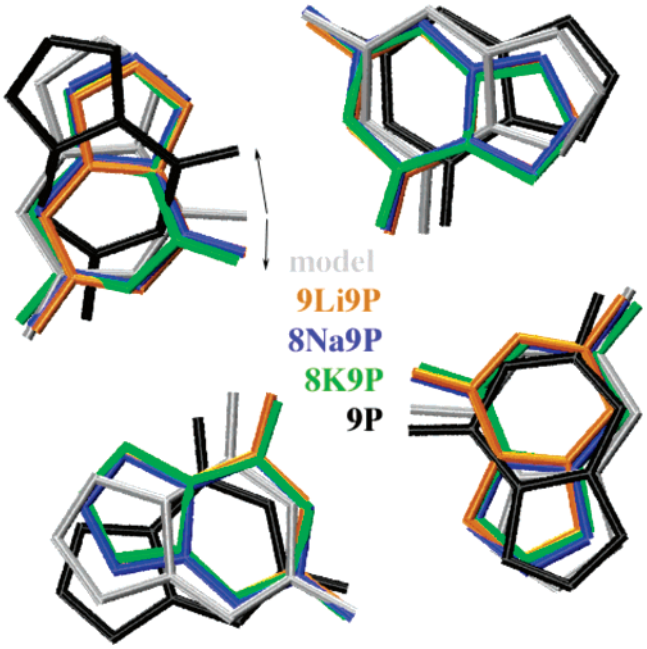

Figure 6. Superposition of the model G4t (gray) with the central G4t of the 9Li9P, 8Na9P, 8K9P, and 9P average structures. The arrows show the rotations of the G-bases, opposite in empty and filled tubes.

increases the quadruplex flexibility (see Figure 7) but also causes a persistent structural deformation, as shown in Figure 3e.

The RMSD and MSD distributions are shown in Figure 4 and are summarized in Table 2. Both the peak central value and its width indicate a higher distortion of the empty 9-plane quadruplex (black line) with respect to those fully coordinated. The same quantities analyzed for 1Li9P (red line) are intermediate between the empty and the saturated channels. These plots clearly indicate, in an unbiased way, that the internal cations assist the stability of the quadruplex conformation also for guanine tetraplexes longer than those investigated in previous studies. We remark that the analysis of the RMSD and MSD is unbiased in the sense that we did not assume a reference-equilibrated structure but the average structure for each G4w. Furthermore, we bypassed the arbitrariness of defining the average structure over a certain time interval by performing within-blocks averages.[32] The agreement between the RMSD and MSD analyses indirectly validates our choice of simulation span to compute the total averages for the RMSD distributions.

Regarding the H-bonds, the combined inspection of Figure 5 and Table 3 reveals that the empty and partially coordinated 9-plane quadruplexes are characterized by a significant deviation of the N2−O7 (external) HBs from the values typical of short-crystallized molecules.[5,33] The internal HBs N1−O6 are instead better preserved. A considerable amount of nonstandard N2−O6 HBs is observed, while N1−N7 HBs are not detected; these trends are opposite to those found in the fully coordinated structures. The in-plane rotation that is responsible for the nonstandard H-bonds occurs in the opposite direction from that experienced by the fully coordinated structures (Figure 6).

The O6−O6 distance chosen to measure the G-channel size in the dynamics of the undercoordinated 9-plane structures varies in the range ∼3 ÷ 6 Å (∼5 ÷ 7 Å) for adjacent (opposite) oxygens with a significant increase relative to the crystallographic values of Figure 1. The average adjacent (opposite) O6−O6 distance is 4.6 ± 1.2 Å (6.4 ± 0.9 Å) for 9P and 4.0 ± 0.9 Å (5.6 ± 1.0 Å) for 1Li9P. The keto oxygens within each G4t are decidedly more distant than in the filled quadruplexes.

In the 1Li9P G4w, the stacking distance between consecutive tetrads varies between 3.2 Å and 3.5 Å with an average value of 3.28 ± 0.04 Å over all of the nine planes (the most frequent value is 3.2 Å and the largest values occur at the borders). In the absence of internal cations, the evaluation of the stacking distances is meaningful only in the range comprising the first 6 planes on the 5′ end, because of major structural deformations on the other end: the values range between 3.4 Å and 3.5 Å, with an average value of 3.46 ± 0.02 Å over the 6 planes on the 5′ end. The average stacking distance in 9P is comparable to the stacking distances at the borders of 1Li9P.

2.5. 20 ns Simulation of the Empty 24-Plane G4w in the Presence of External Li^+ Cations. The results of a longer MD simulation (20 ns) of a longer G4w (Figure 8) allow us to inspect the effects of enhanced stacking interactions on the rigidity of an empty guanine quadruplex. No cations are present in the G-channel at the beginning of the simulation, and the net charge is neutralized by external Li^+ cations. As shown in Figure 8, during the equilibration phase a Li^+ ion gains the G-channel through the 5′ end and adopts a stable intraplane coordination within the G2 tetrad. During the last 5 ns of the simulation, another Li^+ cation adopts an intraplane position in the G17 tetrad reaching the G-channel from the grooves; this approach is most likely favored by the small size of Li ions. A few other lithium cations approach the G-channel from the grooves without going in. A water molecule is constantly positioned above the cation in G2, between the G1 and G2 tetrads; some other water molecules lie near the 5′ terminal during the dynamics. The 3′ terminal is free of cations and several water molecules reach the G-channel at this end and rapidly travel along it thus hydrating the inner core. At the end of the dynamics, the G-channel is almost completely hydrated. No water molecules gain the G-channel through the grooves of the G4w.

The RMSD and MSD distributions are plotted in Figure 4 and summarized in Table 2 for the whole helix (24P, cyan line) and for its central part only (24P*, magenta line), including tetrads from G7 to G18 with G1 being at the 5′ end. The higher mean values and breadths of the distribution peaks reveal a

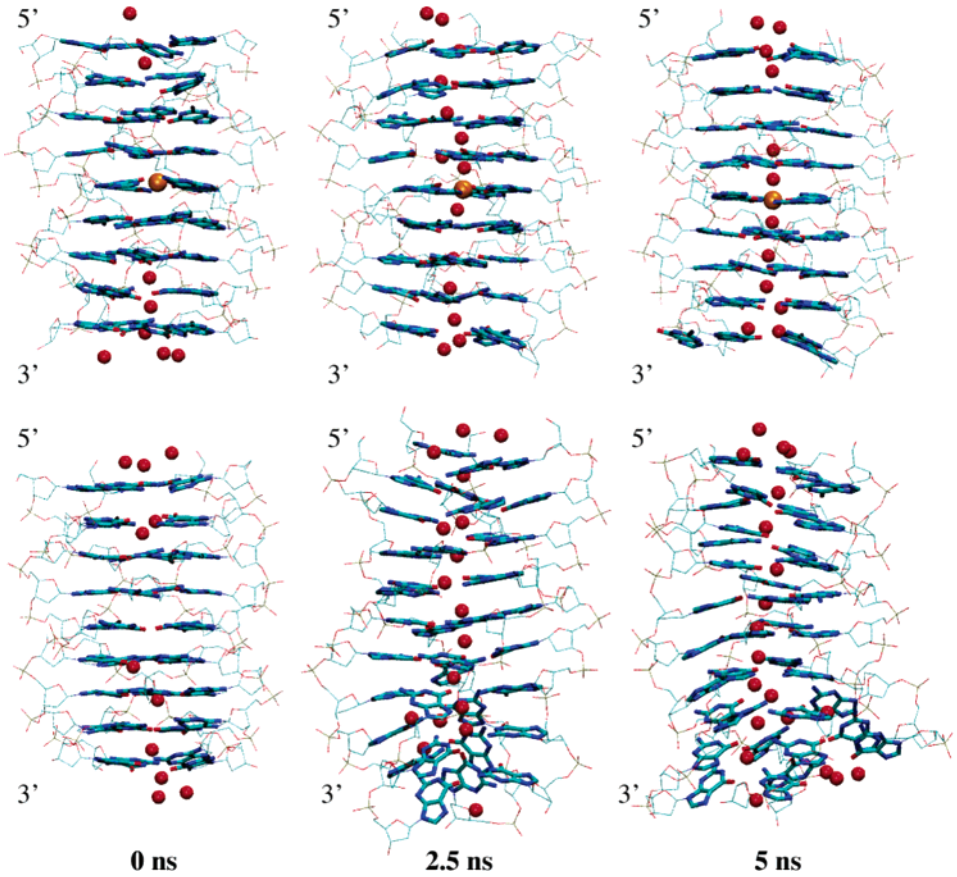

Figure 7. MD snapshots at 0 ns (equilibrated structure), 2.5, and 5 ns of the undercoordinated 9-plane G4w's. Top: the channel contains 1 Li^+ cation (1Li9P, initial geometry in Supporting Figure, S1). Bottom: empty channel (9P). Water molecules inside or approaching the G-channel are represented by red spheres.

major structural flexibility for the undercoordinated long channel, somehow limited in the central part. In fact, the central part 24P* behaves very similarly to the shorter 1Li9P structure. This finding indicates that the longer the quadruplex is, the longer the portion of it is that maintains the regular quadruplex arrangement. In other words, our findings suggest that the collective effect of stacking interactions is conducive to rigid structures.

The HB distributions in Figure 5 and Table 3, compared to the crystallographic values, show that the internal N1—O6 HBs are better preserved than the external N2—N7 HBs. The amount of nonstandard N2—O6 HBs is even higher than that of standard N1—O6 HBs, especially in the inner G4t's (24P*), in which coordinated cations or water molecules are present only in the final part of the simulation. As for 1Li9P and 9P, nonstandard N1—N7 HBs are not observed in this structure.

The adjacent (opposite) O6—O6 distance is 4.5 ± 0.9 Å (6.3 ± 0.9 Å) for 24P and 4.3 ± 0.9 Å (6.1 ± 0.9 Å) for the central part 24P*. Both the adjacent and diagonal O6—O6 distances of 24P are slightly smaller than those detected in 9P in line with the indication noted above of an increasing rigidity with increasing length. The average stacking distance in 24P is 3.3—3.4 Å, slightly lower than in 9P.

2.6. Discussion. *2.6.1. Stability of the G4-Wire Structure as a Function of the Type and Abundance of Internal Cations.* Our simulations show that the presence of many cations inside the G-channel maintains the MD structure of the G4w very similar to the crystallographic one[5,33] with a good preservation of the stacking and coplanarity of the G4t's. The absence of coordinated cations remarkably modifies the original structure and causes evident deformations. Midway between these two extreme behaviors, the decrease of coordinated cations (relative to the saturation condition) increases the quadruplex flexibility and induces border distortions, but on average the G4w maintains the quadruplex symmetry of the starting geometry.

The backbone fluctuations are larger than those of the G-bases in each simulated structure. Analogous results were obtained in other theoretical studies of G4-DNA[14−17] and were explained in terms of poorer accuracy to describe the backbone fluctuations rather than the base fluctuations when using the AMBER/Cornell[22] force field.[42]

The quadruplex in which the guanines fully coordinate the K^+ cations is characterized by a slightly superior structural rigidity in terms of a smaller central value and a smaller amplitude of the RMSD (MSD) peak. Whereas all the considered alkali species give almost equivalent RMSDs for the fully coordinated structures, the analysis of the variance indicates the trend $K^+ > Na^+ > Li^+$ in giving ordered structures. This result is in line with the experimental findings on short guanine tetraplexes[43−45] revealing that cations stabilize the G4w in the order $K^+ > Na^+ > Li^+$. Of course, the atomic MSDs cannot be taken as an index of stability intended as the facility of quadruplex formation with respect to an environment that contains free counterions in solution; to this purpose, the computation of the free energies would be required. Still, the RMSD and MSD reflect the resistance of an intact structural arrangement during the dynamics with small deviations with respect to the average conformation and therefore indicate stability against disruption.

Internal cations also influence the double ring of Hoogsteen HBs characterizing each G4t with the G4t itself undergoing local structural alterations to accommodate cations of different sizes.

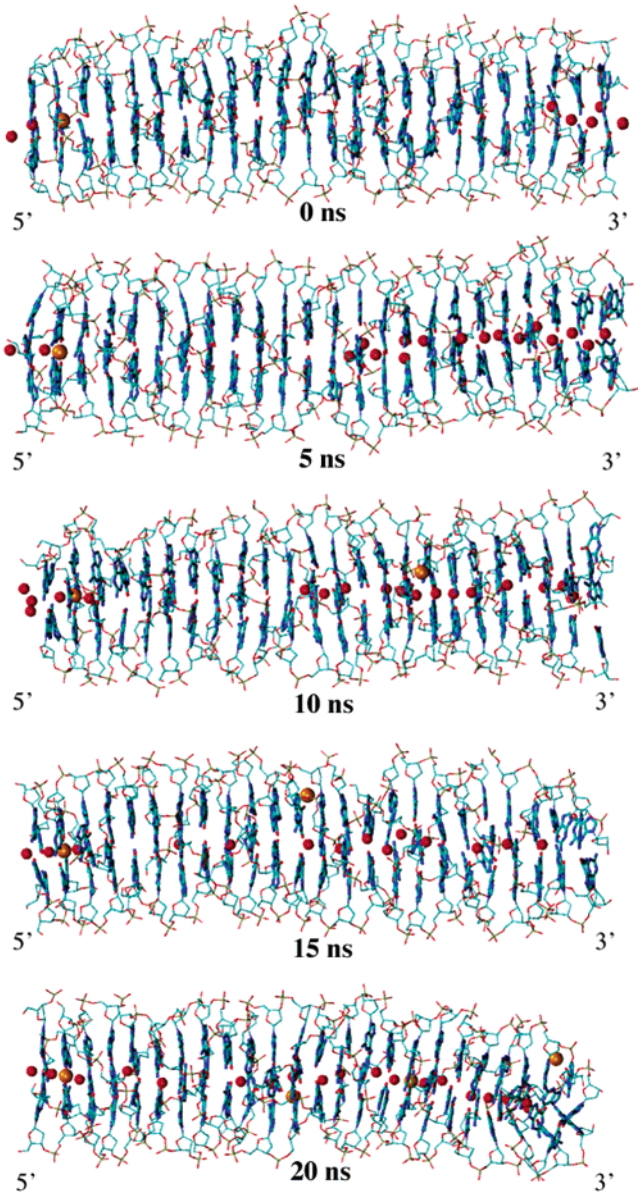

Figure 8. Snapshots at 0, 5, 10, 15, and 20 ns from the MD simulation of the 24-plane G4w (24P) whose starting configuration does not include any internal cations. In addition to the G4w frame, the snapshots also show Li^+ cations (orange spheres) and water molecules (red spheres) that occupy the G-channel during the simulation or are in its close proximity.

In particular, remarkable differences concern the HBs of the outer ring (i.e., the N2—N7 HBs). These interactions are highly preserved in the cation fully coordinated structures, while they experience a strong reduction when only one or no internal cations are present. The decrease of the N2—N7 HBs in the latter structures is combined with the formation of nonstandard N2—O6 HBs, which are responsible for bifurcated N1—O6/N2—O6 contacts, not detected in the cation fully coordinated quadruplexes. The nature of such bifurcated HBs was largely discussed in the past. Spackova and co-workers[14] observed bifurcated HBs in the simulation of a 4-plane guanine quadruplex with three internal Na^+ cations, but they considered these bonds as an artifact of the pair additive nature of the force field. Indeed, we did not find bifurcated N1—O6/N2—O6 HBs in our simulations of the cation fully coordinated G4w's, but only in the undercoordinated structures. Bifurcated HBs in G4w's containing only water molecules inside the G-channel also were observed in the simulation of an initially empty 7-plane parallel G4w[16] in line with our findings. Moreover, in an ab initio quantum chemistry study, Bansal and co-workers[41] showed the formation of bifurcated N1—O6/N2—O6 HBs in the optimized structure of an isolated tetrameric plane.

In the absence of any coordinated cations, even though several water molecules hydrate the G-channel, the repulsion among the electronegative O6 oxygens is not compensated by the positive cation charges; hence, the O6—O6 distances strongly fluctuate during the dynamics. The G-bases in each quartet undergo in-plane rotations to minimize the electrostatic repulsion between adjacent O6 atoms. As a consequence, the O6 oxygen of each base sits almost midway between the N1 and N2 nitrogens of the adjacent guanine, leading to the formation of bifurcated N1—O6/N2—O6 HBs, while several N2—N7 HBs are broken. On the contrary, the distances between adjacent and opposite keto oxygens are maintained around 3.0 and 4.1—4.2 Å, respectively, in the cation fully coordinated G4w's.

2.6.2. Spatial Distribution of Cations inside the G-Channel. Three types of monovalent alkali cations of different sizes were considered: Li^+, Na^+, and K^+. The small radius of the Li^+ ion allows it to coordinate with the four O6 oxygens within the G4t, adopting an intraplane position. The larger Na^+ and K^+ cations are instead preferentially coordinated with the eight keto oxygens belonging to adjacent G4t's, thus preferring an interplane arrangement. The best preservation of the quadruplex arrangement is found with K^+ cations. This "immobility" of the potassium cations is confirmed by NMR[44,46,47] and MD[15] studies. The mobility of Na^+ ions in the G-channel is higher than that of K^+ ions. As described in section 2.3, in a Na^+ cation fully coordinated 9-plane G4w, the central cations maintain the interplane coordination, whereas those closer to the borders move further toward the edges though remaining inside on the simulated time scale. Among the explored alkali species, Li^+ ions have the highest mobility inside the G-channel.

If our investigation is able to reproduce several features and thus to validate the experimental finding that monovalent cations stabilize the tetraplexes in the order $K^+ > Na^+ > Li^+$,[43−45] we do not find clear fingerprints of the well-known ion selectivity sequence $K^+ > Na^+ > Li^+$. Hud and co-workers[12] demonstrated that the preferred coordination of K^+ over Na^+ is driven by the greater energetic cost of Na^+ dehydration with respect to K^+ dehydration. The same conclusion holds for the higher specificity of Na^+ versus Li^+. This explanation substitutes the earlier proposal that the preferential binding of K^+ versus Na^+ (and Na^+ versus Li^+) to the quadruplex was dominated by an optimal fit of K^+ versus Na^+ in the G4w cavity (and Na^+ versus Li^+).[48,49] Our simulations indicate that the ability of the cations to leave the G-channel follows the order $Li^+ > Na^+ > K^+$. This qualitative result is certainly not enough to assess that the relative free energy of hydration dominates the ion selectivity, but it points in that direction.

2.6.3. Stability of the G4w Structure as a Function of the Number of Tetrameric Planes. Our 20-ns MD simulation of an initially empty 24-plane G4w indicates that an increased number of G-planes improves the structural stability. Indeed, we find that the stacking and the coplanarity of the tetrads are better preserved along the whole quadruplex than in the empty 9-plane G4w, including the region where a lithium cation is trapped since the equilibration phase, far from the 5′ terminal. No permanent structural deformations are observed. Moreover, the structural fluctuations of the 12 inner G4t's well compare with those of the 9-plane G4w with one Li^+ cation in the middle of the G-channel, even if no cations reach the center of the helix. It is therefore reasonable to foresee that long G4w's[20] may be

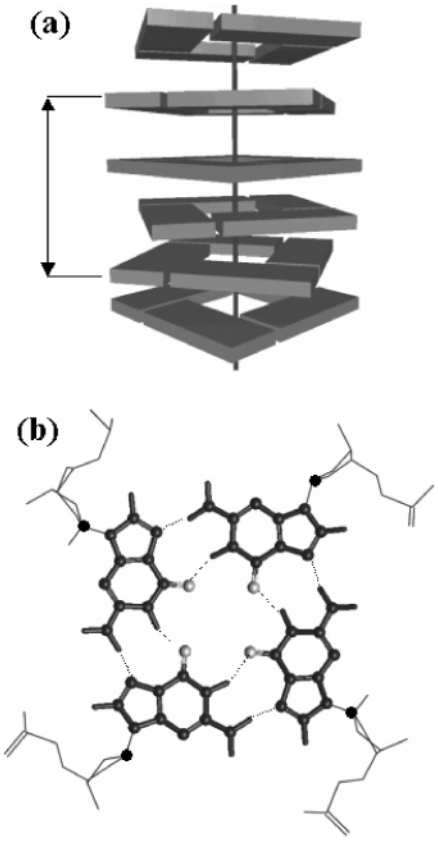

Figure 9. (a) Schematic view of an empty G4-wire. Each plane is represented as a square brick with a central hole to indicate the square symmetry and the collection of 4 identical units (the guanines). The overall appearance is that of an empty tube, inside of which various metals can be hosted. The 3-plane unit building block of the periodic system is identified by the vertical arrow. An atomistic sketch of a tetrameric plane is shown in (b) in which the 8 hydrogen-bonds are clearly marked. Thin sticks represent the attached sugar−phosphate units, not included in the present description and substituted by H atoms (black dots).

stable against unfolding even if a few or no cations are present inside the G-channel.

3. Quantum DFT Calculations

Our first principles calculations[50] are based on DFT[51] with the PBE[52] exchange-correlation functional. The electron−ion interaction is described by ab initio ultrasoft pseudopotentials.[53] The semicore 3s3p electrons of K are included in the valence shell. The semicore shell of Na and Li is instead frozen and taken into account by nonlinear core corrections.[54] The electronic wavefunctions are expanded in plane waves up to a kinetic energy cutoff of 20 Ry. This method was successfully applied for nucleobase assemblies[55,56] and DNA mimics.[57]

Because the helical motif is independent of the interplane backbone linkers and because of our specific interest in the electronic properties of the base stack rather than its decor, we focus on the guanines alone, dropping the surrounding medium and the external attached units (Figure 9). The external groups are replaced by H atoms to saturate dangling bonds, as shown in Figure 9b. Further theoretical investigations about G4-wires[58] and native DNA[59] proved a posteriori that the inclusion of the external backbone does not significantly affect the electronic properties of the systems, at least for the nature of the highest occupied orbitals. The G4-wires are simulated by means of periodically repeated supercells ($24.3 \times 24.3 \times 10.2$ Å^3). The unit supercell contains 3 G4t planes. By taking into account

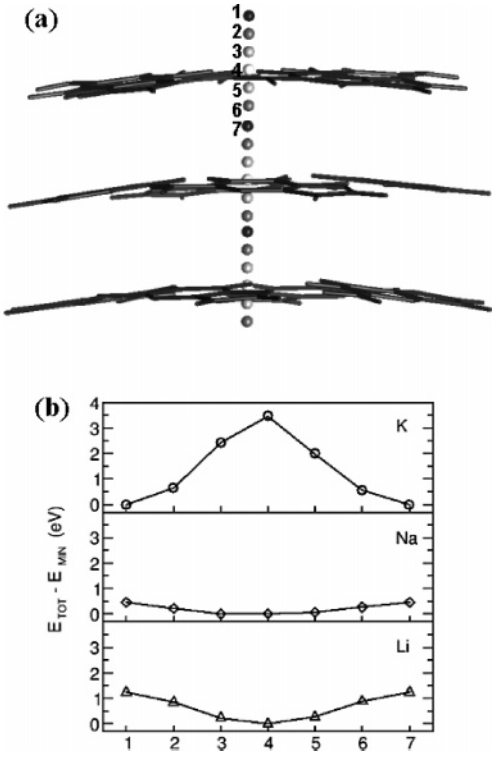

Figure 10. (a) Stick representation of a G4-wire (dark gray frame). Metal ions are located along the axis at different exclusive positions, indicated by the inner spheres of different gray intensities. (b) Relative total energy versus ion location. For each metal species, the origin of the energy scale is fixed at the minimum total energy found for the set of 7 explored sites.

the square symmetry of the G-quartets and the 30° interplane rotation angle, three consecutive planes are sufficient to model the whole helix,[60] with the fourth quartet being the translated image of the first one (Figure 9a). The wires are separated laterally by a thick vacuum layer (∼16 Å) to avoid spurious interactions among neighbor replicas.

The starting atomic positions of the guanines are fixed on the basis of the crystal data pertaining to short four-stranded helices.[5] The inclusion of three metal ions in the central cavity reproduces the cation fully coordinated configurations described in section 2. We consider several configurations, sampling the positions of the ions along the wire, labeled as 1 to 7 in Figure 10a. Positions 1 and 7 mark the interplane site, and position 4 marks the intraplane site. For each monovalent cation (K, Na, Li) and for each selected configuration, we optimize the atomic geometry and the electronic structure. We perform quenched ab initio MD simulations, according to a total energy and force scheme for the search of the local minima.[50] The internal ions are kept fixed, while the guanine atoms are allowed to relax, until the forces vanish within an accuracy of 0.03 eV/Å.

The resulting total energies are shown in Figure 10b. The plot clearly shows that for K^+ ions, the intraplane position is unfavored by ∼3.5 eV with respect to the interplane site that is in agreement with both experimental observations and our MD simulations. The opposite trend is observed for the other two alkali species: Na^+ and Li^+ ions are preferentially hosted in the intraplane positions. We note that the energy barriers of 0.5 eV for Na^+ and 1.2 eV for Li^+ are much smaller than for potassium (Figure 10b). On the basis of the computed energy profiles, we conclude that in agreement with our MD simulations, the Li^+ ions are most likely hosted in the plane of a G4 tetrad, being 4-fold coordinated with the surrounding oxygen atoms. On the other hand, sodium represents an intermediate

case between K and Li: the almost flat energy barrier between the interplane and intraplane sites suggests that Na ions are prone to occupy multiple sites along the helix consistent with the average dynamical structure shown in Figure 3b. This also is consistent with the experimental observation of Na ions in both interplane and intraplane in the X-ray structure.[5,33]

Thus, the first principles calculations give results in qualitative agreement with those of the classical simulations regarding the preferred sites of the different monovalent alkali species. We remark that our DFT calculations neglect some environmental effects that may be of primary importance to determine the quadruplex stability and the ion mobility, such as the temperature, the solvent, the counter-ions, the backbone, etc. Hence, the energy profiles shown in Figure 10b should not be taken as quantitative estimates of the true energy barriers for axial ion migration. However, despite this limitation, they can reliably be exploited to compare the different species, as done above.

4. Summary

We presented the results of classical and quantum calculations performed to investigate G4-wires of different lengths and with different cation concentrations inside them. The main findings concern the issues raised in the discussion of section 2.8.

Alkali ions assist the structural stability in the order of increasing van der Waals radius.

Different alkali species occupy different preferential sites. This result is supported by total energy trends computed within the DFT framework.

Water molecules occupy several viable sites along the backbone, in the channel, and at the openings of the channel, with the accomplishment of a well-defined hydration pattern.

Stacking interactions are a strong stability factor for the quadruplex motif: in fact, long helices formed of several stacked tetrads are resistant against unfolding even without internal cations.

Acknowledgment. We thank Sasha Kotlyar, Danny Porath, Joshua Jortner, Michele Cascella, Paolo Carloni, and Elisa Molinari for fruitful discussions. We are extremely grateful to the anonymous referee for her/his thorough work on the manuscript and the consequent comments that allowed us to improve the content of the article significantly. Funding was provided by the EC under Grant IST-2001-38951, by MIUR-Italy through FIRB-NOMADE, and by INFM−CNR for the allocation of computing time on the parallel super-computers at CINECA (Bologna).

Supporting Information Available: Supporting Information accompanying this article includes a section that reports and discusses a test simulation of a 4-plane G4w, a section that discusses the effects of hydration, and eight figures. The figures describe: (S1) schemes of the starting 9-plane structures; (S2) MD snapshots from the test simulation of the 4-plane G4w; (S3) time evolution of RMSDs; (S4) hydration patterns for the fully coordinated 9-plane 8Na9P quadruplex; (S5) illustration of the sites of external counterions in the case of 9P G4w; (S6−7) histograms of the RMDSs and MSDs for the various investigated G4w's; (S8) X2-test for the variance analysis. This material is available free of charge via the Internet at http://pubs.acs.org.

References and Notes

(1) Gottarelli, G.; Spada, G. P.; Garbesi, A. In *Comprehensive Supramolecular Chemistry*; Atwood, J. L.; Davies, J. E. D.; MacNicol, D.; Vogtle, F., Eds. Pergamon: Oxford, 1996; vol. 9, p 483.

(2) Forman, S. L.; Fettinger, J. C.; Pieraccini, S.; Gottarelli, G.; Davis, J. T. *J. Am. Chem. Soc.* **2000**, *122*, 4060.

(3) Davis, J. T. *Angew. Chem., Int. Ed.* **2004**, *43*, 668.

(4) Kaucher, M. S.; Harrel, W. A., Jr.; Davis, J. T. *J. Am. Chem. Soc.* **2006**, *128*, 38.

(5) Phillips, K.; Dauter, Z.; Murchie, A. I. H.; Lilley, D. M. J.; Luisi, B. *J. Mol. Biol.* **1997**, *273*, 171.

(6) Sessler, J. L.; Sathiosatham, M.; Doerr, K.; Lynch, V.; Abboud, K. A. *Angew. Chem., Int. Ed.* **2000**, *39*, 1300.

(7) Bang, I. *Biochem. Z.* **1910**, *26*, 293.

(8) Gellert, M.; Lipsett, M. N.; Davies, D. R. *Proc. Natl. Acad. Sci. U.S.A.* **1962**, *48*, 2013.

(9) Sen, D.; Gilbert, W. *Nature* **1988**, *334*, 364.

(10) Deng, H.; Braulin, W. H. *J. Mol. Biol.* **1996**, *255*, 476.

(11) These transit times are much longer than those commonly estimated for the natural ion channels. Furthermore, they are also much longer than MD simulation time scales. We do not wish to compare these G-quadruplexes to efficient natural ion channels. Yet, by "ion channel" in this context, we mean a tubular assembly inside of which ions can move along the axis. We also do not wish to sample such a motion by MD, but only to test tendencies to motion and relative behaviors among different ionic species.

(12) Hud, N. V.; Smith, F. W.; Anet, F. A. L.; Feigon, J. *Biochemistry* **1996**, *35*, 15383.

(13) Štefl, R.; Cheatham, T. E, III; Špačkova, N.; Fadrná, E.; Berger, I.; Koča, J.; Šponer, J. *Biophys. J.* **2003**, *85*, 1787.

(14) Špačkova, N.; Berger, I.; Šponer, J. *J. Am. Chem. Soc.* **1999**, *121*, 5519.

(15) Chowdhury, S.; Bansal, M. *J. Biomol. Struct. Dyn.* **2000**, *18*, 11.

(16) Chowdhury, S.; Bansal, M. *J. Phys. Chem. B* **2001**, *105*, 7572.

(17) Chowdhury, S.; Bansal, M. *J. Biomol. Struct. Dyn.* **2001**, *18*, 647.

(18) Rueda, M.; Luque, F. J.; Orozco, M. *J. Am. Chem. Soc.* **2006**, *128*, 3608.

(19) Kotlyar, A. B. private communication. EC project "DNA-Based Nanowires'', http://cordis.europa.eu/ist/fet/openf.htm, Start date May 1, 2006.

(20) Kotlyar, A.; Borovok, N.; Molotsky, T.; Cohen, H.; Shapir, E.; Porath, D. *Adv. Mater.* **2005**, *17*, 1901.

(21) Kale, L.; Skeel, R.; Bhandarkar, M.; Brunner, R.; Gursoy, A.; Krawetz, N.; Phillips, J.; Shinozaki, A.; Varadarajan, K.; Schulten, K. *J. Comp. Phys.* **1999**, *151*, 283.

(22) Cornell, W. D.; Cieplak, P.; Bayly, C. I.; Gould, I. R.; Merz, K. M.; Ferguson, D. M.; Spellmeyer, D. C.; Fox, T.; Caldwell, J. W.; Kollman, P. A. *J. Am. Chem. Soc.* **1995**, *117*, 5179.

(23) Jorgensen, W. L.; Chandrasekhar, J.; Madura, J. D.; Impey, R. W.; Klein, M. L. *J. Chem. Phys.* **1983**, *79*, 926.

(24) Ryckaert, J. P.; Ciccotti, G.; Berendsen, H. J. C. *J. Comput. Phys.* **1977**, *23*, 237.

(25) Essmann, U.; Perera, L.; Berkowitz, M. L.; Darden, T.; Lee, H.; Pedersen, L.G. *J. Chem. Phys.* **1995**, *103*, 8577.

(26) Fletcher, R.; Reeves, C. M. *The Computer Journal* **1964**, *7*, 149.

(27) The external ions were added in a shell around the G4w using a coulombic potential on a grid of 1 Å resolution to roughly minimize the electrostatic energy. The initial positions of the water molecules reproduced a snapshot from a room temperature equilibration for the TIP3P model.

(28) Berendsen, H. J. C.; Postma, J. P. M.; van Gunsteren, W. F.; DiNola, A.; Haak, J. R. *J. Chem. Phys.* **1984**, *81*, 3684.

(29) Kolb, A.; Dünweg, B. *J. Chem. Phys.* **1999**, *111*, 4453.

(30) Nose, S. J. *Chem. Phys.* **1984**, *81*, 511.

(31) Kneller, G. R. *Mol. Simul.* **1991**, *7*, 113.

(32) Maragliano, L.; Cottone, G.; Cordone, L.; Ciccotti, G. *Biophys. J.* **2004**, *86*, 2765−2772.

(33) Laughlan, G.; Murchie, A. I. H.; Norman, D. G.; Moore, M. H.; Moody, P. C. E.; Lilley, D. M. J.; Luisi, B. *Science* **1994**, *265*, 520.

(34) Pearlman, D. A.; Case, D. A.; Caldwell, J. W.; Ross, W. R.; Cheatham, T. E., III; DeBolt, S.; Ferguson, D.; Seibel, G.; Kollman, P. *Nature (London)* **1992**, *356*, 126.

(35) Špačkova, N.; Berger, I.; Egli, M.; Šponer, J. *J. Am. Chem. Soc.* **1998**, *120*, 6147.

(36) Strahan, G. D.; Keniry, M. A.; Shafer, R. H. *Biophys. J.* **1998**, *75*, 968.

(37) Špačkova, N.; Berger, I.; Šponer, J. *J. Am. Chem. Soc.* **2001**, *123*, 3295.

(38) Štefl, R.; Špačkova, N.; Berger, I.; Koča, J.; Šponer, J. *Biophys. J.* **2001**, *80*, 455.

(39) Fadrna, E.; Špačkova, N.; Štefl, R.; Koča, J.; Cheatham, T. E., III; Šponer, J *Biophys. J.* **2004**, *87*, 227.

(40) Pearlman, D. A.; Case, D. A.; Caldwell, J. W.; Ross, W. R.; Cheatham, T. E., III; DeBolt, S.; Ferguson, D.; Seibel, G.; Kollman, P. *Comput. Phys. Commun.* **1995**, *91*, 1.

(41) Gu, J.; Leszczynski, J.; Bansal, M. *Chem. Phys. Lett.* **1999**, *311*, 209.

(42) Hobza, P.; Kabelac, M.; Šponer, J.; Mejzlik, P.; Vondrasek, J. *J. Comput. Chem.* **1997**, *18*, 1136.

(43) Hardin, C. C.; Watson, T.; Corregan, M.; Bailey, C. *Biochemistry* **1992**, *31*, 833.

(44) Xu, Q.; Deng, H.; Braunlin, W. *Biochemistry* **1993**, *32*, 13130.

(45) Guschlbauer, W.; Chantot, J. F.; Thiele, D. *J. Biomol. Struct. Dyn.* **1990**, *8*, 491.

(46) Deng H.; Braunlin, W. *J. Mol. Biol.* **1996**, *255*, 476.

(47) Hardin, C. C.; Corregan, M. J.; Lieberman, D. V.; Brown, B. A., II. *Biochemistry* **1997**, *36*, 15428.

(48) Sundquist, W. I.; Klug, A. *Nature (London)* **1989**, *342*, 825.

(49) Williamson, J. R.; Raghuraman, M. K.; Cech, T. R. *Cell* **1989**, *59*, 871.

(50) Baroni, S.; Dal Corso, A.; de Gironcoli, S.; Giannozzi, P. http://www.pwscf.org. "Plane-Wave Self-Consistent Field" package, version 2.1.3, released on April 20, 2005.

(51) Dreizler, R. M.; Gross, E. K. U. "Density Functional Theory. An approach to the quantum many-body problem"; Springer-Verlag: Berlin, 1990.

(52) Perdew, J. P.; Burke, K.; Ernzerhof, M. *Phys. Rev. Lett.* **1996**, *77*, 3865.

(53) Vanderbilt, D. *Phys. Rev. B* **1990**, *41*, 7892.

(54) Louie, S. G.; Froyen, S.; Cohen, M. L. *Phys. Rev. B* **1982**, *26*, 1738.

(55) Di Felice, R.; Calzolari, A.; Molinari, E.; Garbesi, A. *Phys. Rev. B* **2002**, *65*, 045104.

(56) Calzolari, A.; Di Felice, R.; Molinari, E.; Garbesi, A. *Physica E* **2002**, *13*, 1236.

(57) Zhang, H.; Calzolari, A.; Di Felice, R. *J. Phys. Chem. B* **2005**, *119*, 15345.

(58) Di Felice, R.; Calzolari, A.; Garbesi, A.; Alexandre, S. S.; Soler, J. M. *J. Phys. Chem. B* **2005**, *109*, 22301.

(59) Gervasio, F. L.; Carloni, P.; Parrinello, M. *Phys. Rev. Lett.* **2002**, *89*, 108102.

(60) Calzolari, A.; Di Felice, R.; Molinari, E.; Garbesi, A. *Appl. Phys. Lett.* **2002**, *80*, 3331.